AD 700 030

INTERIOR BALLISTICS AND GUN FLASH AND SMOKE

H. L. Brode, et al

RAND Corporation
Santa Monica, California

October 1969

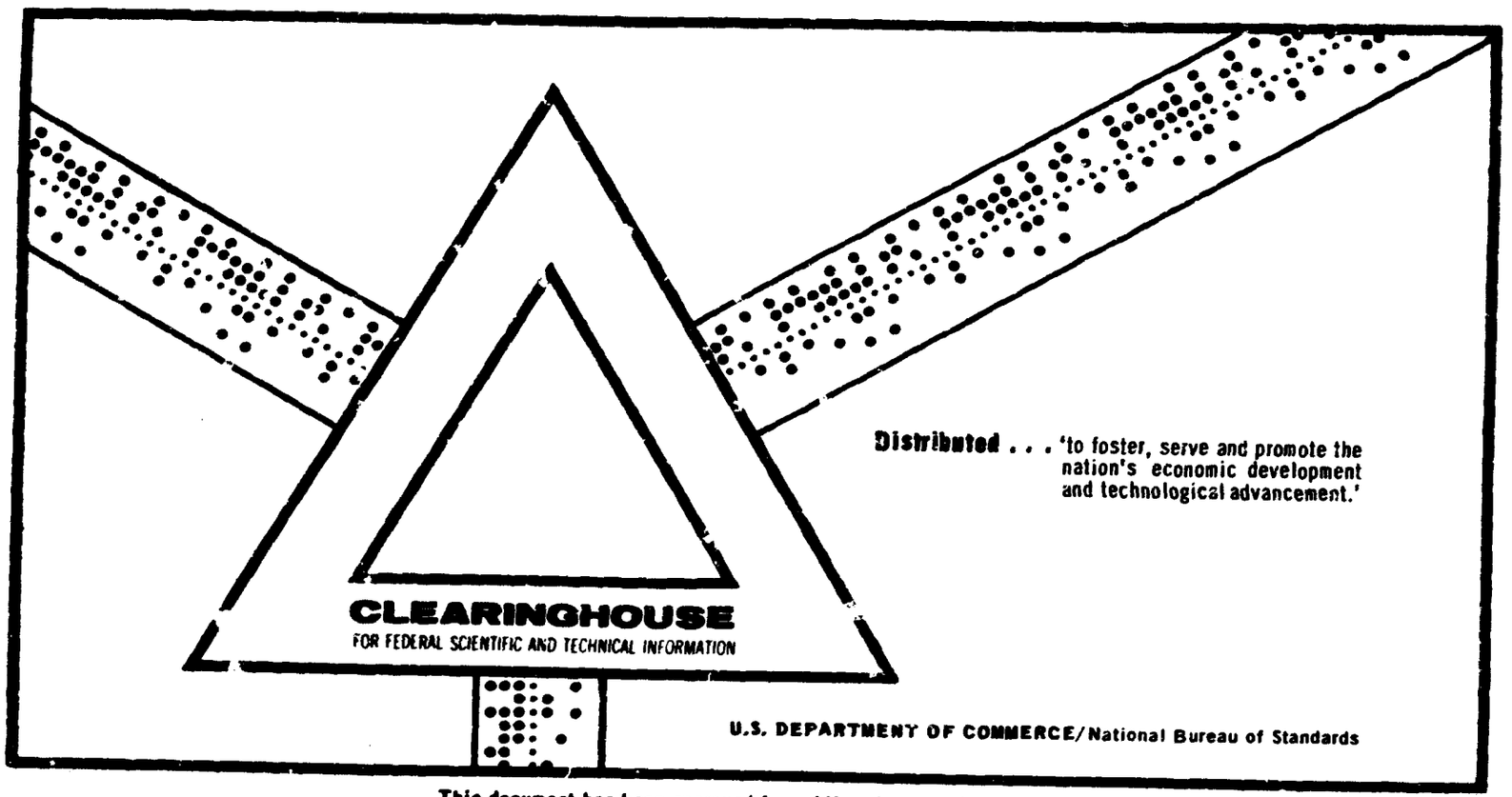

This document has been approved for public release and sale.

AD700030

MEMORANDUM
RM-6127-PR
OCTOBER 1969

INTERIOR BALLISTICS AND GUN FLASH AND SMOKE

H. L. Brode and J. E. Enstrom

DDC
FEB 4 1970
B

PREPARED FOR:

UNITED STATES AIR FORCE PROJECT RAND

The RAND Corporation
SANTA MONICA • CALIFORNIA

THIS DOCUMENT HAS BEEN APPROVED FOR PUBLIC RELEASE AND SALE; ITS DISTRIBUTION IS UNLIMITED.

44

MEMORANDUM

RM-6127-PR

OCTOBER 1969

INTERIOR BALLISTICS AND GUN FLASH AND SMOKE

H. L. Brode and J. E. Enstrom

This research is supported by the United States Air Force under Project RAND—Contract No. F44620-67-C-0045 monitored by the Directorate of Operational Requirements and Development Plans, Deputy Chief of Staff, Research and Development, Hq USAF. Views or conclusions contained in this study should not be interpreted as representing the official opinion or policy of the United States Air Force.

DISTRIBUTION STATEMENT

This document has been approved for public release and sale; its distribution is unlimited.

The RAND Corporation

PREFACE

Large and small calibre guns have long been important tools of warfare and still are. A detailed understanding of the gas dynamics in a discharged gun could be of great help in the design of new guns, shells or charges. Such knowledge is also important to efforts to suppress or detect gun smoke, gun flash, and gun blast. The work reported on in this memorandum was prompted by a need for quantitative data on temperatures and densities in the gun exhaust pertinent to detection by radar or infrared scanning devices. Dr. William G. McMillan first directed our attention to this problem, and we are further indebted to him for suggesting sources for experimental data.

The methods are developed here for interior ballistics. Calculations of this sort are capable of modeling gun performance well enough to be an important supplement to empirical gun tests and charge firing trials. In addition, some understanding of gun flash, blast, and smoke have been gained by extensions of these methods.

We are greatly indebted to the personnel of the U.S. Naval Weapons Laboratory, Dahlgren, Virginia (principally Dave Bowen, with the cooperation of Frank Kasdorf) for the collection and interpretation of gun characteristics and firing sequence data used for inputs to and comparison with our calculations.

Helpful discussions with Alan Shapiro here at Rand are also acknowledged as is the prior interest in this subject by Jack Craig. We would also like to thank Wakichi Asano for his valuable programming assistance.

This work represents a progress report, since the authors can foresee further investigations of charge characteristics, energy losses in the barrel, and other non-ideal effects, as well as a more detailed hydrodynamical model of the smoke and flash. Expressions of interest in such extensions and criticisms of the work presented here are welcomed.

SUMMARY

This paper considers the gas dynamics of various large naval guns, including the interior ballistics (charge burning, propellant gas expansion and shell acceleration) and the nature of the gas expansion and air shock beyond the muzzle. Solutions are accomplished by a numerical program which integrates the partial differential equations appropriate to the gas dynamics in one space dimension. The equations of state for the gas and the air are treated in some detail, as is the nature of the charge burn, the barrel friction, and the shell inertia. The dynamics of the partially burned charge gases which sometimes flash burn after ejection from the muzzle are treated within the limits of expansion into various conical geometries. Comparisons are made with observations of both the interior ballistics and of the smoke, flash and blast from the exhaust.

TABLE OF CONTENTS

I. INTRODUCTION

This paper introduces an accurate numerical method for obtaining the hydrodynamic properties associated with the propellant gas as it moves down a gun barrel and exhausts to the air. Previous analytical solutions to this problem have found it necessary to make a number of simplifying assumptions and approximations, some of which limit the accuracy and range of applicability of the results. Even the very recent treatment of high speed guns by A. E. Seigal[1] takes no account of the nature of the propellant and simply assumes that it burns instantly into an ideal gas with constant specific heat. Further, Seigal assumes that the shell moves without any frictional or heat losses. By far the most extensive treatment of interior ballistics is by J. Corner.[2] He summarizes all important work in the field before 1950. The "isothermal" solution is the simplest and it assumes that the propellant burns according to a specified law into a gas which expands isothermally during burning with a constant specific heat ratio which is increased from that of an ideal gas to account for heat losses. The shell mass is increased to account for frictional resistance.

Generally, in Corner's theory, in order to arrive at the correct peak breech pressure, muzzle velocity, pressure-time history, and shell ejection time for a given gun, the solution is made to depend on three propellant parameters, the burning law, the total energy released, and the rate of burning. Corner describes a more detailed solution which takes account of the temperature dependence of the gas and includes a number of other small corrections. It leads to very complicated analytical expressions which depend basically on a propellant burning law parameter and a burning rate parameter. Corner shows a few cases where good agreement with experimental values can be obtained by proper adjustment of the parameters. Each gun must be treated separately and the solution is very sensitive to the various adjusted parameters.

The treatment we present here takes good account of many of the factors in the problem which previously suffered from simplifying assumptions. Using a full partial differential formulation of the gas dynamics simplifies some factors which have only a minor effect on the

PRECEDING PAGE BLANK

results and reduces interior ballistic problems to a single free parameter, namely the propellant burning rate. This parameter is obtained for one gun by fitting to experimental data and the solution for peak chamber pressure, muzzle velocity, pressure-time history, and shell ejection time is then shown to be accurate to the order of ten percent for several different guns.

Previous descriptions of gun flash and smoke have almost entirely been qualitative in nature and no rigorous mathematical treatment is known to exist. The hydrodynamical solution which we present, while limited in its thoroughness by a number of simplifying assumptions, does reproduce quantitatively a number of properties observed in actual guns, such as, the pressure as a function of time and distance from the muzzle and the shock reheating of the gas outside of the gun.

II. INTERIOR BALLISTICS

In the results presented here are examples for six different naval guns ranging in size from 5"/38 caliber to 16"/50 caliber. The physical characteristics of these guns are listed in Table 1.[3] The table includes such parameters as chamber volume, propellant weight, shell weight, and shell travel distance. All the propellants used in these guns are essentially identical. They consist of roughly 90% nitrocellulose, 2-3% butyl stearate, 1% ethyl centralite, 1% lead carbonate, 1% potassium sulphate, 3% volatiles, and 1-2% moisture. They come in the form of cylindrical grain roughly of diameter d_o and length $\ell \simeq 2d_o$, with roughly six web perforations of diameter $w_p \simeq .1d_o$. Values for these quantities are also given in Table 1.

In this analysis of interior ballistics, we have made the following simplifying assumptions: (1) each gun is unworn so that no gas leaks between the shell and the barrel; (2) the only losses in the system are frictional in nature; (3) the pressure drop needed to overcome the "skin friction" of the barrel in moving the gas down the barrel is negligible; (4) gun recoil and the energy expended in shell rotation are negligible; (5) the chamber can be replaced by a cylindrical continuation of the barrel with the same total volume; and (6) the propellant grain distributes itself uniformly between the breech and shell during its burning. These assumptions can be shown to be consistent with the general accuracy of our method.[4] Other conditions necessary in formulating the solution are discussed below.

MATHEMATICAL FORMULATION

The equations which describe the interior ballistics part of the calculation are one-dimensional since the cross section is assumed to be uniform along the length of the gun. The equation of motion in Lagrangian form is

$$\frac{\partial u}{\partial t} = -\frac{\partial}{\partial m}(P + Q) \qquad (1)$$

where $u = u(x,t) = \frac{\partial X(x,t)}{\partial t}$ is the velocity of the gas in meters/milli-

Table 1

GUN AND PROPELLANT PARAMETERS

Gun	V_{ch} (m^3)	M_{sh} (Mg)	W_{prop} (Mg)	D_o (m)	A (m^2)	L_{ch} (m)	L_{trav} (m)	R_{tot} (m)	ρ_o (Mg/m^3)	d_o (m)	ℓ (m)
5"/38	.0107	.0251	.00741	.127	.0127	.84	4.10	4.94	.696	.0056	.011
5"/54	.0130	.318	.00885	.127	.0127	1.03	5.96	7.00	.680	.0069	.012
6"/47	.0241	.0590	.0171	.152	.0182	1.32	6.13	7.45	.712	.010	.022
8"/55 (Mark 15)	.0781	.152	.0440	.203	.0324	2.41	9.61	12.02	.563	.011	.025
8"/55 (Mark 16)	.0552	.152	.0377	.203	.0324	1.70	9.87	11.58	.683	.013	.028
16"/50	.443	1.23	.297	.406	.130	3.41	17.52	20.93	.671	.024	.053

second; X(x,t) is the Eulerian coordinate which gives the position, at time t, of a gas element that was initially at position x, the Lagrangian coordinate; $m = m(x,t) = \int_0^x \rho(x,t)dx$ is the mass of the gas in megagrams/meter^2; $\rho = \rho(x,t)$ is the density in megagrams/meter^3; $P = P(x,t)$ is the pressure in jerks/meter^3 (1 jerk = 10^{16} ergs or 1 jerk/meter^3 = 10^4 bars), and

$$Q = Q(x,t) = \frac{C_1(\Delta m)^2}{V} \left| \frac{\partial V}{\partial t} \right|^2 + \frac{C_2 \Delta m}{V} \left| \frac{\partial V}{\partial t} \right| \text{ for } \frac{\partial V}{\partial t} < 0 \qquad (2)$$

and $\quad = 0$ for $\frac{\partial V}{\partial t} \geq 0$,

is an artificial viscosity pressure introduced [5,6] to remove mathematical discontinuities which would otherwise occur whenever compressions lead to shock waves in the gas. Typical values appropriate to this problem are $C_1 = 6.0$ and $C_2 = 0.5$. Δm is a mass element and $V = V(x,t) = 1/\rho(x,t)$ is the specific volume of the gas in meters^3/megagram.

The equation of energy conservation is

$$\frac{\partial E}{\partial t} = -(P + Q)\frac{\partial V}{\partial t} + B(P,f) \qquad (3)$$

where $E = E(x,t)$ is the internal energy density of the gas in jerks/megagram and $B(P,f)$ is a source term which represents the rate at which energy is being added to the gas by the burning of the propellant. B can be written as a function of pressure (P) and of the fraction of propellant already burned (f).[7]

For most propellants the burn rate in energy per unit time (B_t) is known to be directly proportional to the exposed propellant surface area (S) and the gas pressure on the propellant (P), or

$$B_t = cSP \qquad (4)$$

where c is a constant. This relationship has been verified for nitrocellulose,[8] although at pressures near atmospheric P should be replaced by $a + bP$, where a and b are constants.

For the cylindrical grain described earlier, neglecting the burning of the ends and the webbing as a first approximation, we can write S as a function of f and other known constants. For the fraction of total propellant burned as a function of time we can write

$$f = f(t) = 1 - \frac{\pi d^2 \ell/4}{\pi d_o^2 \ell/4} = 1 - \frac{d^2(t)}{d_o^2} \tag{5}$$

Now we assume that the propellant of total weight W_{prop} consists of n grains each of weight W_n and density ρ_n, so

$$W_{prop} = nW_n = n\rho_n V_n = n\,\rho_n\,\pi d_o^2 \ell/4 \tag{6}$$

and

$$S = nS_n = n\pi d\ell = \frac{4\,W_{prop}\,d}{\rho_n d_o^2} \tag{7}$$

so, using Eq. (5),

$$B_t = c\,\frac{4W_{prop}\,d}{\rho_n d_o^2}\,P = c\,\frac{4W_{prop}}{\rho_n d_o}\,(1-f)^{1/2}\,P \tag{8}$$

Thus we can write B(P,f) in energy per unit mass per unit time as

$$B(P,f) = s\,(1-f)^{1/2}\,P \tag{9}$$

where $s = c\,\frac{4W_{prop}}{\rho_n}\,\frac{1}{d_o} \approx .01\ m^4/Mg\text{-}ms/d_o$. The numerical value .01 has been estimated, independent of W_{prop} and ρ_n, from burning rate data[8] and then modified to give a better fit to the experimental data, as will be discussed later. Also, we assume our nitrocellulose propellant has a calorific value, $E_{prop} \approx 1000$ cal/gm = 4.2 jerks/Mg.[9]

The equation of motion of the shell is obtained by using the velocity and pressure of the gas at the shell boundary as it moves down the barrel:

$$M_{sh}\frac{du(x_{sh},t)}{dt} = P(x_{sh},t)\,A - F_{fr} \tag{10}$$

where A is the cross sectional area of the barrel and F_{fr} assumes that

all the energy lost in the motion of the shell is caused by a frictional force acting between the shell and the barrel which is directly proportional to the pressure on the shell (appropriate for a fluid on a deforming plastic seal or metal shell):

$$F_{fr} = fr \cdot P(x_{sh},t)\ A. \tag{11}$$

Eq. (10) can be rewritten as follows:

$$\frac{du}{dt} = \frac{PA}{M_{sh}}(1 - fr) = \frac{PA}{M_{eff}} \tag{12}$$

where $M_{eff} = \frac{M_{sh}}{(1-fr)} = M_{sh} + M_{sh}\frac{fr}{1-fr}$.

The fraction of kinetic energy of the shell going into frictional energy loss is thus fr/(1-fr). Corner suggests that this fraction is roughly twenty percent.[10]

Other models for the dissipative force were tried but seemed to be much poorer in terms of physical soundness and resultant solutions. One such alternate scheme assumed the frictional force, Eq. (11), was a constant and another subtracted energy from Eq. (3) as a function of the kinetic energy of the shell.

In an effort to derive an appropriate caloric equation of state for nitrocellulose we have relied on the similarities obvious in the Chapman-Jouguet adiabatics for other explosives,[11] as we were unable to find any experimental detonation data for nitrocellulose. In Figure 1 we have plotted $\gamma - 1$ vs ρ for TNT with loading density ρ_o = 1.50 gm/cm^3 [12] and for Pentolite with ρ_o = 1.65 gm/cm^3. [13] By fitting a smooth curve to this data in the region of interest, namely, $\rho \leq$ .5 gm/cm^3, we obtain

$$\gamma(\rho) - 1 \simeq \frac{.09 + 2\rho^2}{.3 + \rho^2} \tag{13}$$

Nitrocellulose propellant generally has a loading density $\rho_o \simeq .7$ gm/cm^3. This lower initial density prompted a somewhat arbitrary

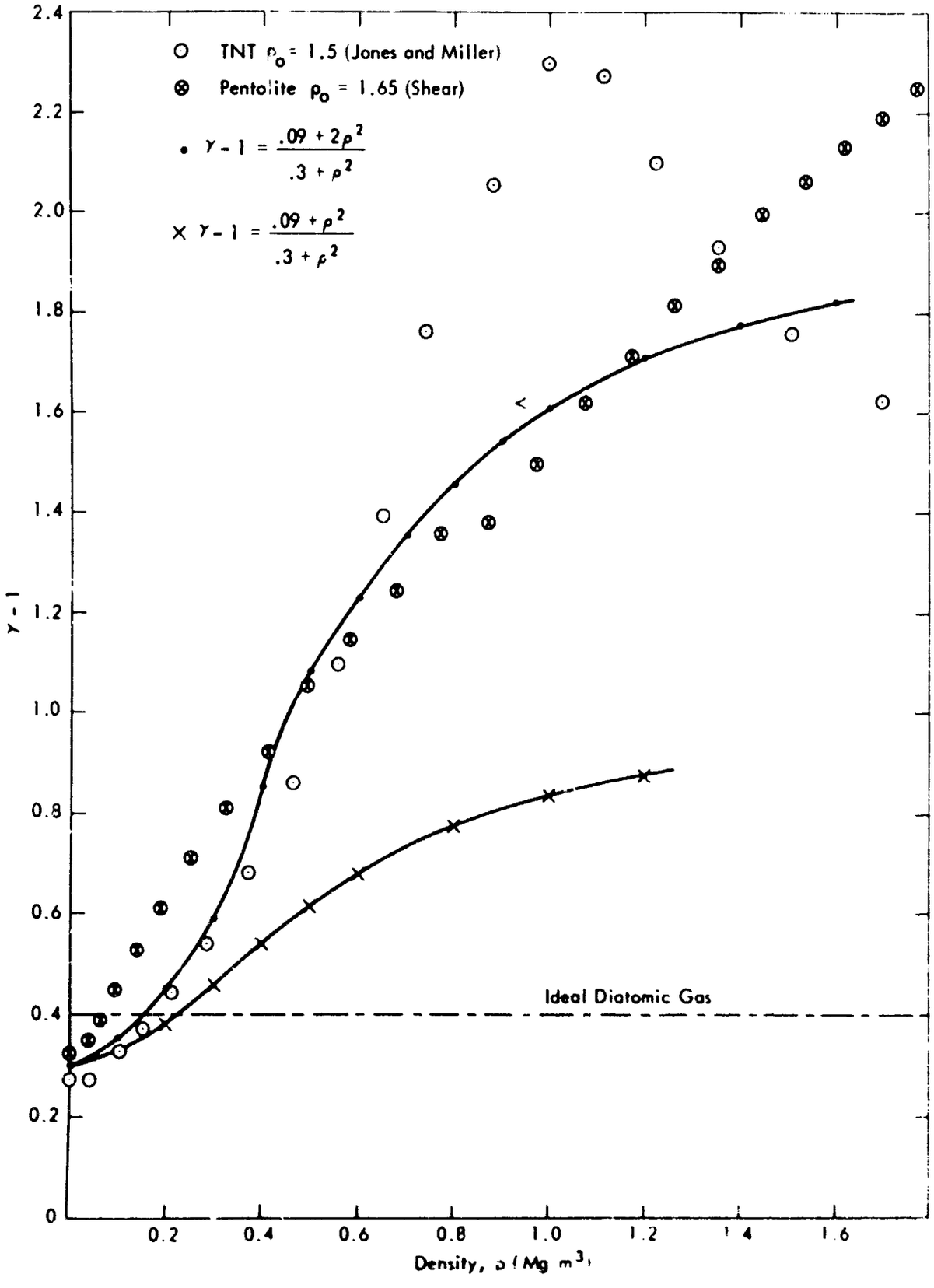

Fig. 1—Caloric equations of state

modification to the fit:

$$\gamma(\rho)-1 \simeq \frac{.09 + \rho^2}{.3 + \rho^2} \tag{14}$$

using the fact that the value of $\gamma(\rho)-1$ in the high density limit ($\rho \gg 1$ gm/cm^3) has been shown to be linearly related to loading density. The formulation of this result by Miller,[14] based on explosives, shows that we can write

$$\gamma(\infty)-1 = \frac{1}{3} + G\,\rho_o/\rho_c \tag{15}$$

where ρ_o is the loading density of the explosive, ρ_c is its crystalline density, and G is a constant determined by the Morse atomic parameters associated with each of the elements composing the explosive. An independent determination by Fickett and Wood,[15] using various thermodynamic relationships, along with experimental data on the thermal equation of state and detonation velocity for various explosives, leads to empirical results for $\gamma(\infty)-1$ similar to Eq. (15). The transition from the high density region to the low density region of the gas is obtained by using Eq. (14).

Thus our caloric equation of state is

$$P = E\rho[\gamma(\rho)-1] \simeq E\rho\left(\frac{.09 + \rho^2}{.3 + \rho^2}\right) \tag{16}$$

For low densities, $\rho \ll .1$ gm/cm^3, Eq. (16) describes an ideal gas of $\gamma = 1.30$. The effect on the results of varying the density dependence of $\gamma(\rho)-1$ has been investigated and is reviewed in the Results and Discussion Section.

The thermodynamic description of the gas is completed by using a thermal equation of state of the form

$$T = (M/R)\ (P/\rho)\ /\ (1 + \beta(\rho)) \tag{17}$$

where R is the Rydberg gas constant, M is the average molecular weight

of the propellant gas (about 30 gm/mole), and $\beta(\rho)$ is a "covolume" correction [16, 17] to the ideal gas law, which is roughly linear in density and about 1.-2. at ρ = .5 gm/cm^3, depending on the exact form of the correction used.

NUMERICAL SOLUTION

A solution for the hydrodynamic functions in this problem results from numerical integration of the two equations of motion, Eqs. (1) and (12), the energy equation, Eq. (3), and the caloric equation of state, Eq. (16). These can be written in difference equation form as follows:

$$u_j^{n+1/2} = u_j^{n-1/2} - \frac{\Delta t^n}{\Delta m_j}\left[P^n_{j+1/2} - P^n_{j-1/2} + Q^{n-1/2}_{j+1/2} - Q^{n-1/2}_{j-1/2}\right] \quad (18)$$

$$u^{n+1/2}_{j\ max} = u^{n-1/2}_{j\ max} + \frac{A}{M_{sh}} P^n_{j\ max}\,(1\text{-fr}) \quad (19)$$

$$E^{n+1}_{j-1/2} = E^n_{j-1/2} - \left[\tfrac{1}{2}(P^{n+1}_{j-1/2} + P^n_{j-1/2}) + Q^{n+1/2}_{j-1/2}\right](V^{n+1}_{j-1/2} - V^n_{j-1/2}) + s\,P^n_{1/2}\left(1 - \left[\left(\sum_{i-1}^{n} E^i_{1/2}\right)/E_{prop}\right]\right)^{1/2} \quad (20)$$

$$P^{n+1}_{j-1/2} = E^{n+1}_{j-1/2}\,\rho^{n+1}_{j-1/2}\left[.09 + (\rho^{n+1}_{j-1/2})^2\right]/\left[.3 + (\rho^{n+1}_{j-1/2})^2\right] \quad (21)$$

with

$$X^{n+1}_j = X^n_j + u^{n+1/2}_j\,\Delta t^{n+1/2} \quad (22)$$

$$Q^{n+1/2}_{j-1/2} = \frac{2C_1(\Delta m_{j-1/2})^2\,(V^{n+1}_{j-1/2} - V^n_{j-1/2})^2}{(V^{n+1}_{j-1/2} + V^n_{j-1/2})(\Delta t^{n+1/2})^2} + \frac{2C_2\,\Delta m_{j-1/2}\,\left|\,V^{n+1}_{j-1/2} - V^n_{j-1/2}\,\right|}{(V^{n+1}_{j-1/2} + V^n_{j-1/2})\,\Delta t^{n+1/2}} \quad (23)$$

$$\text{for } V^{n+1}_{j-1/2} < V^{n}_{j-1/2}, \text{ with } V^{n+1}_{j-1/2} = \frac{X^{n+1}_{j} - X^{n+1}_{j-1}}{\Delta m_{j-1/2}} \tag{24}$$

where $n \geq 1$ and $1 \leq j \leq j_{max}$. The mass elements $\Delta m_{j-1/2}$ are fixed initially and remain unchanged throughout the solution. Notice that in writing the source term of Eq. (20) we have used the pressure and energy density of the breech. The pressure and energy density are not actually uniform throughout the gas, but as discussed later, these approximations have a negligible effect on the results.

Unit increments in the superscript n represent step-wise increments in time and unit increments in the subscript j represent finite increments in the mass, corresponding to a spatial zone, where $j = 1$ is the zone at the beginning of the chamber and $j = j_{max}$ is the zone adjacent to the shell. The integration is performed by advancing in time (n) with the step size determined by stability conditions which depend on the local sound speed in the gas and the artificial viscosity.[18] Then for each step in time, we obtain a complete hydrodynamical description of the propellant gas by advancing in mass zone from $j = 1$ to $j = j_{max}$. These equations yield a self-consistent solution for u, E, ρ, P as functions of time and position, with T determined independently from ρ and P.

By using the loading density and an initial energy density of the propellant assuming atmospheric temperature, we specify gas conditions in the chamber. The constants fr, which determines the effective mass of the shell, E_{prop}, the energy/mass released from the propellant, and s, the rate of propellant burning must also be specified. From previous discussion, we know fr = .2, E_{prop} = 4.2 jerks/Mg, and s = .01/d_e. These values are used initially and then modified to obtain the best possible results. The effect of varying these parameters is discussed in the results.

RESULTS AND DISCUSSION

In Table 2 we present for each of the six guns which we have studied the best fit values for the three quantities, u_{muz}, the shell

Table 2

SUMMARY OF BEST FIT RESULTS

Gun	s_1 ($\approx .01/d_o$)	s	u_{muz} (m/ms)		P_{max} (jerk/m^3)		τ_{ej} (ms)	
			Calcul.	Exp.	Calcul.	Exp.	Calcul.	Exp.
5"/38	1.82	1.78	.75	.78	.32	.30	9.8	
5"/54	1.48	1.48	.75	.77	.31	.30	13.5	13.5
6"/47	1.03	1.06	.72	.76	.33	.31	15.5	
8"/55 (Mark 15)	.94	1.04	.79	.77	.35	.35	23	24
8"/55 (Mark 16)	.80	.90	.75	.76	.34	.34	23	
16"/50	.43	.46	.70	.73	.32	.30	45	

muzzle velocity, P_{max}, the peak breech pressure and τ_{ej}, the shell ejection time, along with the corresponding experimental values. In Figure 2, we present calculated and experimental pressure-time curves for the 5"/54 gun. All solutions were obtained using fr = 0, and $E_{prop} = 4.2$. We used s = 1.48 for the 5"/54 gun and then computed $s^i = .01/d_o^i$ as an estimate for the other guns. The actual value of s used along with s^i are shown in Table 2. The results show agreement between the best fit values and experimental values to be better than 5% in most cases and better than 10% in all cases.

In Table 3 we present a summary of the efficiency of guns. There are two standard measures of efficiency. The first is called "piezometric efficiency" and is defined as the average pressure necessary to accelerate the shell to the observed muzzle velocity divided by the peak breech pressure. We compute the average pressure $\bar{P}$ as follows from Eq. (13), with fr = 0,

$$\bar{P} A = M_{sh} a = M_{sh} \frac{(u_{muz}^2)}{2 R_{tot}} \tag{25}$$

or

$$\bar{P} = \frac{1/2 M_{sh} u_{muz}^2}{A R_{tot}} \tag{26}$$

where R_{tot} is the combined chamber length, L_{ch}, and shell travel length, L_{trav}. Piezometric efficiencies are usually about .4 - .5.[19] We see from Table 3 that the efficiencies for these guns are somewhat lower than this.

The second measure is "ballistic efficiency," and is defined as the ratio of the kinetic energy of the shell at muzzle velocity to the energy of the propellant. We shall calculate this efficiency in two ways: first we shall use the full energy/mass of the propellant, $E_{prop} = 4.2$ jerks/Mg, and second we shall use the energy/mass actually burned at the time of shot ejection, $E_{prop}(\tau_{ej})$. Both these efficiency values along with $E_{prop}(\tau_{ej})$, are shown in Table 3. The typical ballistic efficiency of 1/3[19] lies roughly between our two sets of calculated values. The maximum possible ballistic efficiency for these guns, obtained if the charge is completely burned before the shot moves appreciably, can be shown to be roughly 1/2.[19]

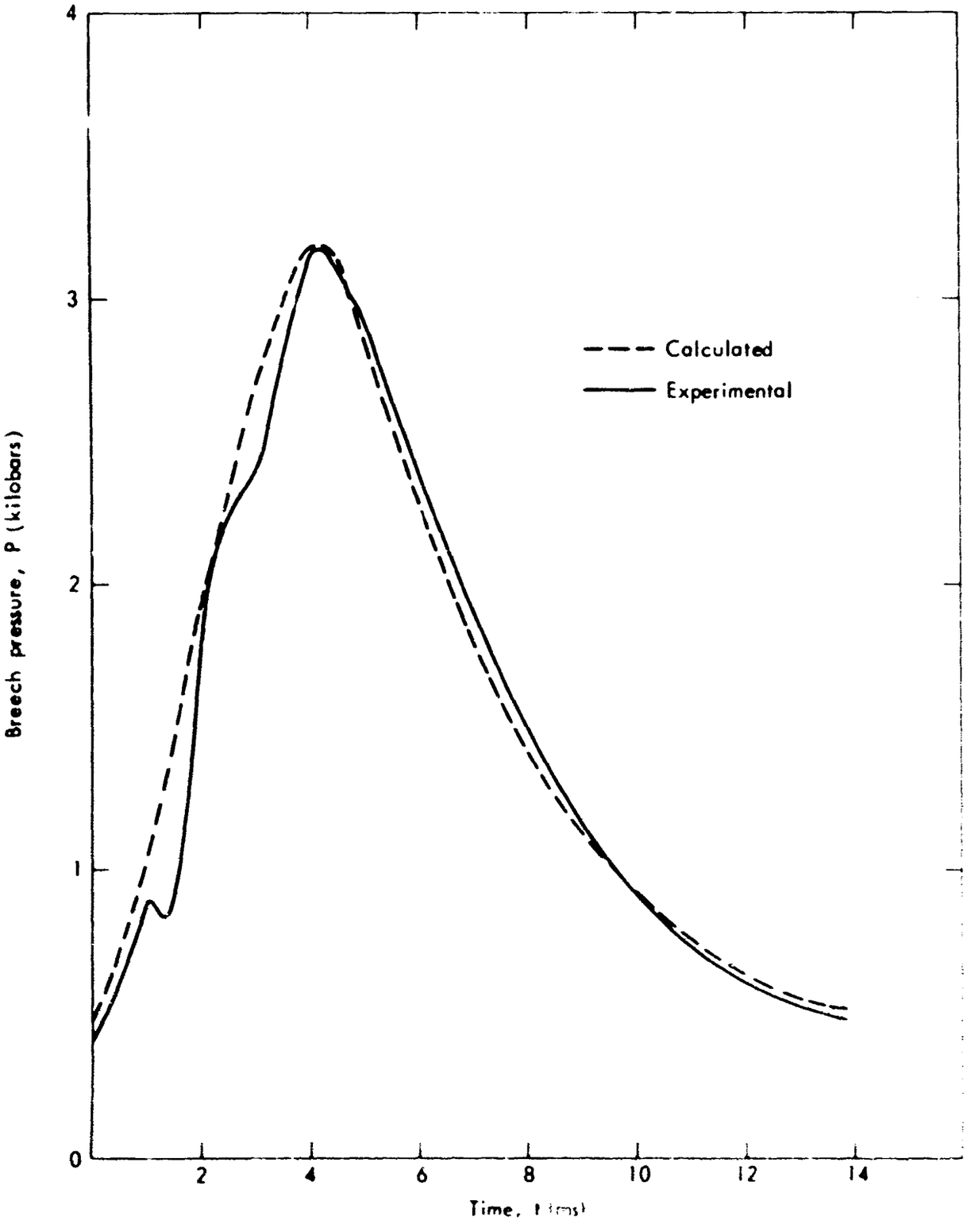

Fig. 2—Pressure-time history for 5"/54 gun

Table 3

BALLISTIC EFFICIENCIES

Gun	Shell Kinetic Energy $1/2\ M_{sh}\ u_{muz}^2$ (jerks)	$E_{prop}(\tau ej)$ (jerks/Mg)	Ballistic Efficiency using E_{prop}	Ballistic Efficiency using $E_{prop}(\tau ej)$	Piezometric Efficiency
5"/38	.00762	2.5	.245	.411	.411
5"/54	.00945	2.7	.254	.452	.351
6"/47	.0171	2.4	.238	.416	.407
8"/55(Mark 15)	.0449	3.2	.243	.319	.327
8"/55(Mark 16)	.0442	3.0	.279	.391	.343
16"/50	.327	2.5	.262	.440	.406

In order to interpret the significance of these results, we must discuss the changes caused by varying the parameters in the problem. These changes were obtained by keeping fixed all parameters but the one whose affect we are studying, and then obtaining solutions for several values of this parameter. Changing fr from .0 to .25 decreases u_{muz} by less than 4% and increases P_{max} by about 25%, with the changes in u_{muz} and P_{max} roughly linear with the changes of fr. Changing E_{prop} from 4.2 to 3.0 jerks/Mg without changing s, decreases u_{muz} by about 3% and increases P_{max} about 1%. One reason that this change has so little effect is that for E_{prop} = 4.2 jerks/Mg the propellant is only about 60-75% burned at τ_{ej}, and lowering the value of E_{prop} to 3.0 jerks/Mg simply increases the fraction of propellant burned at τ_{ej}. Lowering E_{prop} still further would then begin lowering u_{muz} and P_{max} quite strongly. The fact that the nitrocellulose propellant we have used is only partially burned at τ_{ej} indicates that it most likely has a calorific value less than 1000 cal/gm. Modifying the form of $\gamma(\rho)-1$ from Eq. (14) so that it goes from the minimum of .3 at low density to a maximum which is 1.2, increases u_{muz} by about 10% and P_{max} by about 20%. The shape of pressure-time history is somewhat less sensitive to changes in $\gamma(\rho)-1$ but if the maximum value is raised significantly above 1.0, the peak in the curve occurs sooner than 1/3 τ_{ej} and if the maximum value is much lower than 1.0, then the peak occurs at roughly 1/2 τ_{ej}. The results are fairly dependent on $\gamma(\rho)-1$ but we have chosen an expression which we believe to be most accurate.

After we have established values for fr, E_{prop}, and $\gamma(\rho)-1$, as discussed earlier, the quantity s is our only variable parameter. We study the effect its variation has on u_{muz} and P_{max} for each of the guns. Using the fixed conditions fr = 0. and E_{prop} = 4.2, with $\gamma(\rho)$ given by Eq. (14) and with B(P,f) given by Eq. (9), a curve of u_{muz} versus s is shown in Figure 3 and a curve of P_{max} versus s is shown in Figure 4.

Combining Figure 3 and Figure 4 and plotting peak breech pressure versus muzzle velocity in Figure 5 it is seen that as the burn rate increases the pressure rises much more rapidly than the velocity. This reflects the fact that as the burn rate increases the pressure builds up faster to a larger peak value, while the amount of energy put into the gas approaches the total energy in the charge.

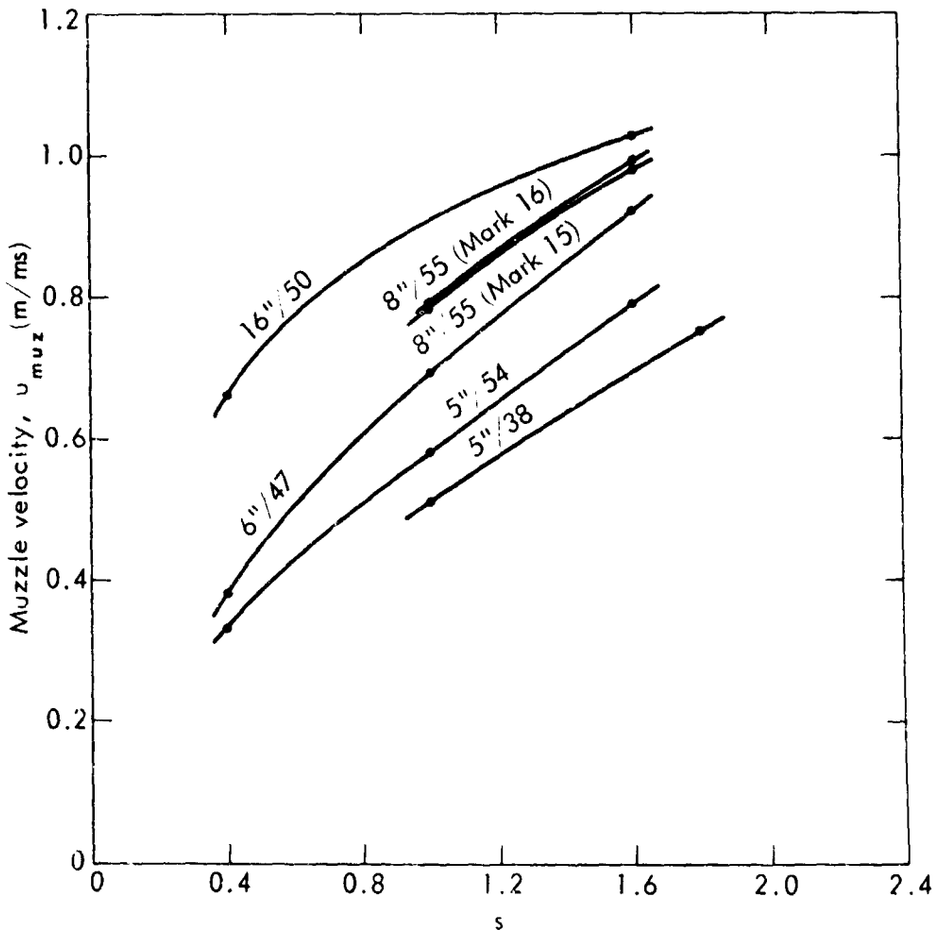

Fig. 3—Muzzle velocity versus burning rate

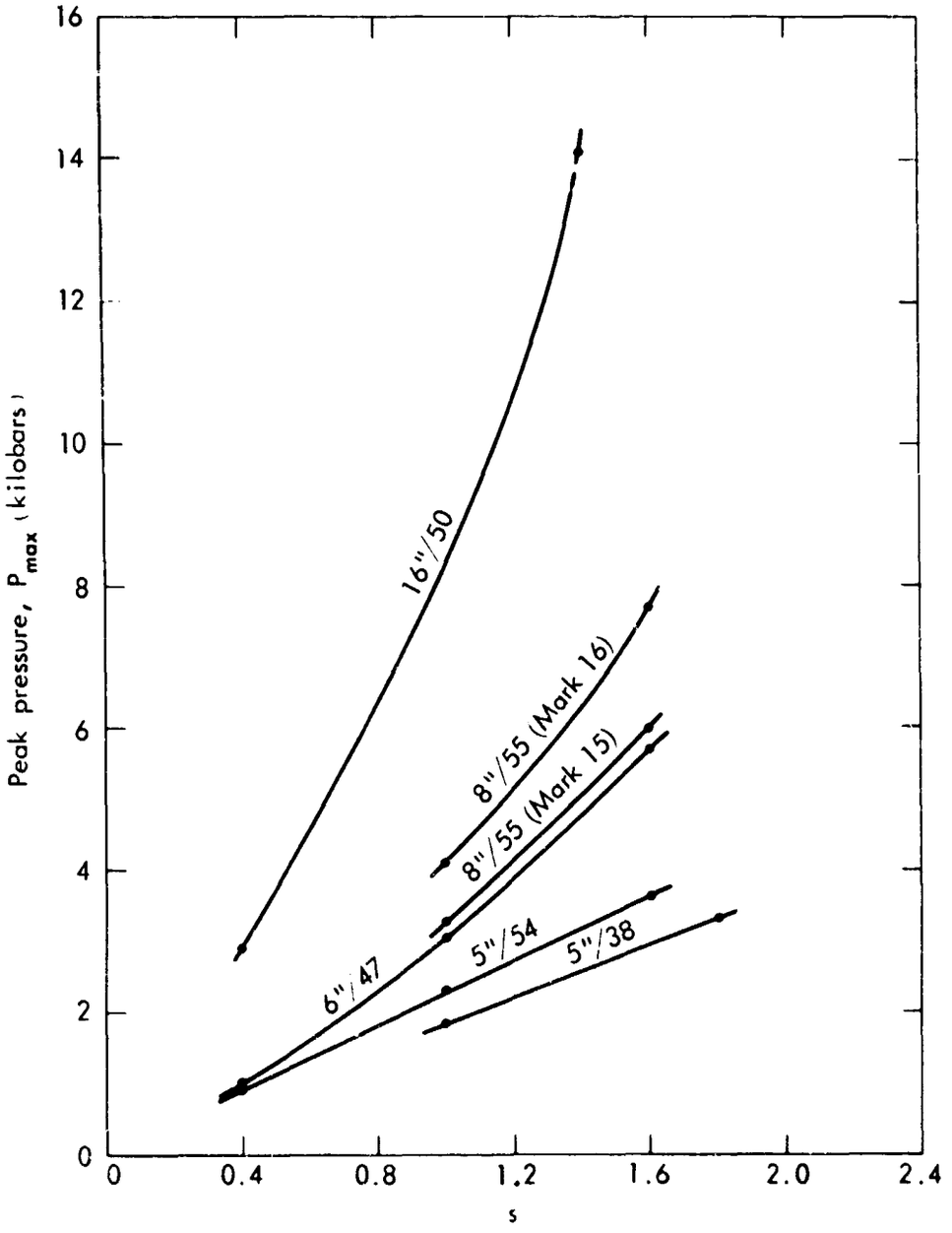

Fig. 4—Peak pressure versus burning rate

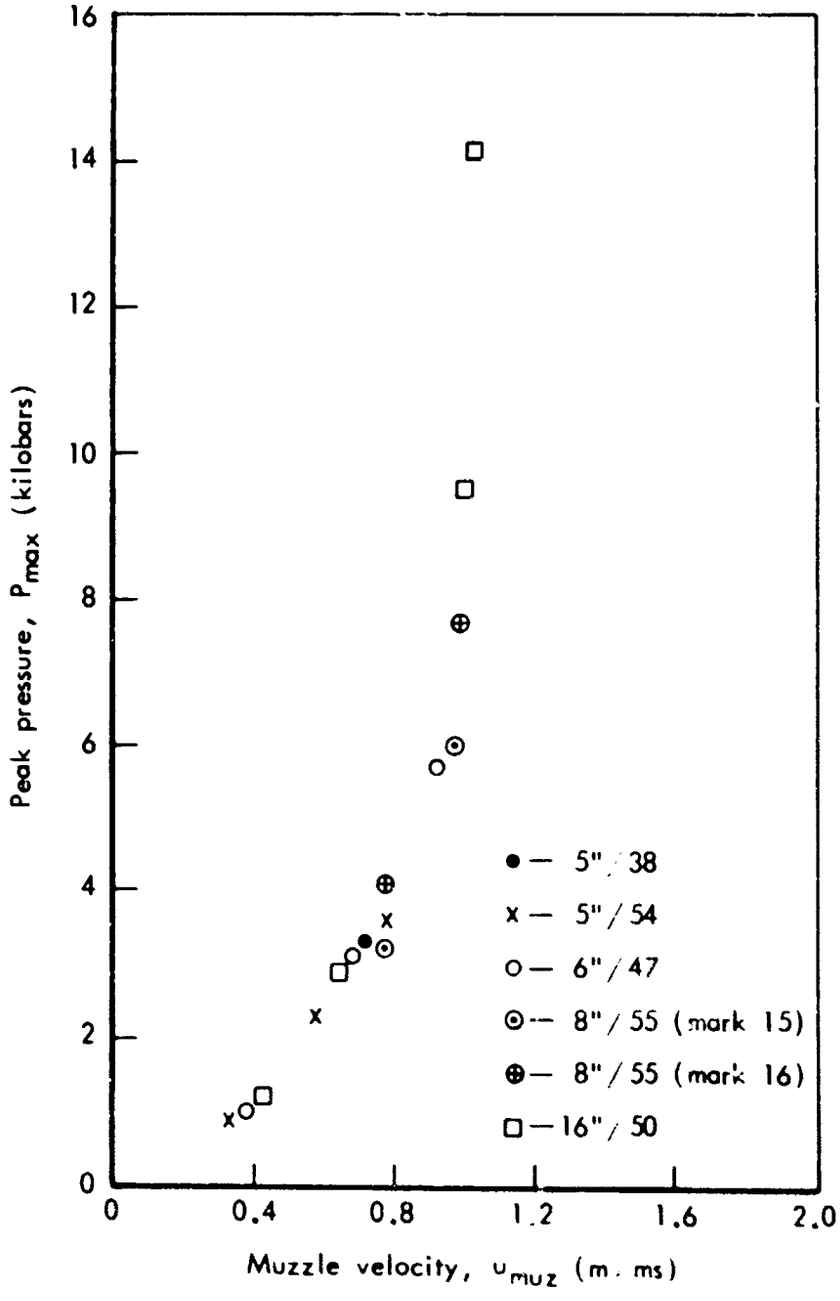

Fig. 5—Peak pressure versus muzzle velocity

We have also investigated using burning laws of the form $B(P,f) = s\,P^{\alpha}(1-f^{\gamma})$ where $.8 \leq \alpha < .1$ and $2 \leq \gamma \leq 10$ and have found that u_{muz} and P_{max} are not particularly sensitive to α and γ as long as s is adjusted to keep the burning rate roughly the same. As mentioned earlier, we have also made calculations using individual zone pressure and energy instead of breech pressure and energy, and these yield the same results as long as s is adjusted slightly to keep the overall burning rate the same. In addition we have investigated burning the propellant according to Eq. (10) only in the chamber part of the gun. We have found that for a fixed value of s, burning only in the chamber vs. burning all the way between the breech and the shell leaves P_{max} approximately the same and decreases u_{muz} by about 10%.

As a further study on the nature of the burning, we have initially ignited only the first 20% of the propellant. This is done by setting the initial energy density of all but the first 20% equal to zero and then letting the hydrodynamical calculations propagate the ignited gas down through the remaining propellant. The result of this is to create shock waves in the gas which propagate between the shell and the breech. The magnitude and time dependence of the resultant oscillations in breech pressure depends critically on the fraction of propellant initially ignited and also on the burning law for the remaining propellant. We believe that this initial burning process thus accounts for the oscillations which are observed in the actual pressure-time histories. However, since we do not know the precise experimental details of the ignition process, we have retained the original assumption of uniform burning as a good first-order approximation, consistent with accuracy of our other assumptions.

As a final study we have investigated the effects of mass ablation and turbulant heat transfer on our results. These energy loss effects are treated independently of the frictional losses and require modification of the equations of motion and energy. In the Appendix we give a detailed description of the new equations and show that the results are only slightly affected by the changes.

III. FLASH AND SMOKE

We now treat the propellant gas as it exits from the muzzle. The gas composition is such that it usually forms a combustible mixture with the surrounding air and a momentary flash of bright light results from a shock-initiated burn. Based on our survey of available experimental data[3] and on previous studies,[20] the flash phenomenon can be divided into basically three regions. The first two regions are muzzle glow, a small region of low luminosity at the muzzle, and the primary flash, a high-luminosity region which is separated from the muzzle glow by a dark region. These regions are usually discernible only for small guns. For the large guns which we are considering, the third region, or secondary flash, is a highly luminous continuation of the primary flash and occupies most of the gas volume.

The cause of the flash phenomenon has been explained qualitatively. Basically, the gas expands and cools very rapidly upon leaving the muzzle, and consequently the luminosity diminishes and the dark region results. This gas is then recompressed through a decelerating shock, which raises the temperature back up to roughly the muzzle temperature and forms the luminous primary flash which is relatively small and usually lasts for a few milliseconds. In the meantime air has mixed with the unburned hydrogen and carbon monoxide in the muzzle gas, forming a combustible mixture. The exact composition of the muzzle gas is highly dependent on such parameters as the initial loading density of the propellant and the final density of the gas,[12] besides being dependent on the original propellant composition. If the temperature of the recompressed gas is above the ignition temperature of the combustible mixture or if a piece of burning propellant penetrates the gas cloud, then it will burn and form the large secondary flash. The occurrence of flash is often inhibited by the presence of certain substances, such as potassium sulphate, which act as suppressants. If the unburned propellant gas is only partially ignited or not ignited at all, then it appears as smoke outside of the gun.

In order to form a hydrodynamical model of the flash phenomenon we will make a number of assumptions which simplify the calculations:

(1) the muzzle gas emerges into a radially symmetric conical section, which is initially a full hemisphere and then steadily decreases to a very narrow angle cone; (2) the emerging muzzle gas displaces the surrounding air and no explicit account is taken of any mixing between the two; (3) the unburned propellant remains uniformly mixed throughout the gas, but the chemical composition of the gas itself is not determined or used in the calculations; (4) the emerging propellant gas obeys Eq. (14) and the surrounding air is treated as an ideal diatomic gas of specific heat ratio $\gamma = 1.4$. Although these assumptions are quite restrictive, we still expect to gain certain quantitative information about the nature of the flash phenomenon.

MATHEMATICAL FORMULATION

The numerical solution now separates into two parts. The interior ballistics are still governed by the previously described equations of motion and caloric equation of state. For the expansion into air we have the equation of motion

$$\frac{\partial u}{\partial t} = - r^2 \frac{\partial}{\partial m_F} (P + Q_F) \tag{27}$$

where r, the radial distance from the muzzle, now replaces X, the linear distance used in Eq. (1), $M_F = 4\pi F \int_0^r \rho(r,t) r^2 dr = \frac{4\pi F}{3} \rho r^3$ is the total mass in an Fth of a sphere where $F \leq 1$, $m_F = M_F/4\pi = \frac{F}{3}\rho r^3$ is corresponding mass per steradian. We can write $F = \sin^2 \frac{\theta}{2}$ where θ is the angle between the axis and the boundary defining the cone into which the gas is expanding, and Q_F is the modified artificial viscosity

$$Q_F = Q_F(r,t) = \frac{C_3 (\Delta m_F)^2}{V r^4} \left| \frac{\partial V}{\partial t} \right|^2 + \frac{C_4 \Delta m_F}{V r^2} \left| \frac{\partial V}{\partial t} \right| \text{ for } \frac{\partial V}{\partial t} < 0 \tag{28}$$

where C_3 and C_4 are constants and Δm_F is a mass element.

The energy equation outside the gun becomes

$$\frac{\partial E}{\partial t} = - (P + Q_F) \frac{\partial V}{\partial t} + SR \tag{29}$$

where SR is a source term which represents the burning of the gas. We shall arbitrarily assume that SR can be written as a function of gas temperature T in a form similar to Eq. (9),

$$SR = c(1 - f)^{1/2} T \tag{30}$$

where c is a constant which will be adjusted so that the gas will be completely burned about 10 milliseconds after first exiting from the muzzle. T is obtained by using the thermal equation of state, Eq. (17), which reduces to the ideal gas law at the low densities outside of

the gun. The air surrounding the gas does not burn and so we set SR = 0. in that region.

The caloric equation of state for the gas is given by Eq. (16) and the equation for air is

$$P = .4E\rho \tag{31}$$

The approximation of air as an ideal gas is valid for the relatively low temperatures and densities which occur in the flash region.

NUMERICAL SOLUTION

We can now write Eq. (27) to (31) in difference equation form

$$u_j^{n+1/2} = u_j^{n-1/2} - \frac{\Delta t^n (r_j^n)^2}{\Delta m_{Fj}} \left[P^n_{j+1/2} - P^n_{j-1/2} + Q_F{}^{n-1/2}_{j+1/2} - Q_F{}^{n-1/2}_{j-1/2} \right] \quad (32)$$

$$E^{n+1}_{j-1/2} = E^n_{j-1/2} - \left[\frac{1}{2}(P^{n+1}_{j-1/2} + P^n_{j-1/2}) + Q_F{}^{n+1/2}_{j-1/2}\right] (V^{n+1}_{j-1/2} - V^n_{j-1/2}) + SR^n_{j-1/2}\, \Delta t^n \quad (33)$$

$$P^{n+1}_{j-1/2} = .4\, E^{n+1}_{j-1/2}\, \rho^{n+1}_{j-1/2} \quad (34)$$

where, in the gas region,

$$SR^n_{j-1/2} = 2\, \tau^n_{j-1/2} \left(1. - \left(\sum_{i=1}^{n} E^i_{j-1/2}\right)/E_{tot}\right)^{1/2} \quad (35)$$

and where

$$Q^{n+1/2}_{Fj-1/2} = \frac{2C_3 (\Delta m_{Fj-1/2})^2 (V^{n+1}_{j-1/2} - V^n_{j-1/2})^2}{(V^{n+1}_{j-1/2} + V^n_{j-1/2})\, (\Delta t^{n+1/2})^2\, A(r^{n+1})^2} + \frac{2C_4\, \Delta m_{Fj-1/2}\, |V^{n+1}_{j-1/2} - V^n_{j-1/2}|}{(V^{n+1}_{j-1/2} + V^n_{j-1/2})\, (\Delta t^{n+1/2})\, A(r^{n+1})} \quad \text{for } V^{n+1} < V^n \quad (36)$$

and

$$\Delta m_{Fj-1/2} = \frac{B(r^{n+1})}{V^{n+1}_{j-1/2}} \quad (37)$$

with

$$A(r^{n+1}) = \left(\frac{r^{n+1}_j + r^{n+1}_{j-1}}{2}\right)^2 \quad \text{for } r^{n+1}_{j-1} > D_o/2 \quad (38)$$

$$= \left(\frac{r_j^{n+1} + D_o/2}{2} \right)^2 \quad \text{for } r_{j-1}^{n+1} < D_o/2 \text{ and } r_j^{n+1} > D_o/2$$

and

$$B(r^{n+1}) = \frac{4\pi F \left[(r_j^{n+1})^3 - (r_{j-1}^{n+1})^3 \right]}{3} \quad \text{for } r_{j-1}^{n+1} > D_o/2 \qquad (39)$$

$$= \frac{4\pi F \left[(r_j^{n+1})^3 - (D_o/2)^3 \right]}{3} + \frac{\pi D_o^2}{4} \left(\frac{D_o}{2} - r_{j-1}^{n+1} \right) \quad \text{for } r_{j-1}^{n+1} < \frac{D_o}{2} \text{ and}$$

$$r_j^{n+1} > \frac{D_o}{2}$$

where D_o is the gun barrel diameter.

The solution is obtained by defining the origin as the center of the muzzle and supplying as initial data the velocity, pressure, density, and temperature of the propellant gas as a function of negative distance from the muzzle, $r_j^n \equiv X_j^n - R_{tot}$ for $0. \leq X_j^n \leq R_{tot}$ and $1 \leq j \leq j_{max}$ at the time when the shell reaches the muzzle. The numerical integration uses Eqs. (18), (20), (21), (22), (23), and (24) for the plane geometry region $r_j^n > D_o/2$, where Eqs. (38) and (39) give the appropriate geometrical factors for the transition between the two regions.

The initial conditions for the air outside the gun are obtained by assuming standard temperature ($T = .03 \times 10^4$ °K) and pressure ($P = 9.5 \times 10^{-5}$ jerks/m^3).

These calculations were carried out for the 5"/54 gun as a representative case and one for which we have comparable experimental data.

RESULTS AND DISCUSSION

A survey of several dozen firings of the 5"/54 gun, as recorded on 16mm film taken at 96 frames/sec,[3] shows flash and smoke characteristics which are in good agreement with the general description given earlier. The gas initially emerges into a full hemisphere ($\theta = \pi/2$, $F = 1/2$), after about 10 milliseconds it emerges into a cone of angle $\theta \simeq \pi/3$ ($F = 1/4$), and after about 20 milliseconds it emerges into a cone of angle $\theta \simeq \pi/4$ ($F = 1/8$). After about 50 milliseconds the gas is emerging straight forward, which it continues to do until it is completely exhausted about 100 milliseconds later.

In the firings where there is no flash, the initially emitted gas forms a large cloud of smoke roughly two meters long and two meters wide which drifts away from the muzzle slowly, and through this is shot the gas which emerges at a smaller angle and forms a second cloud of smoke further downstream. In the firings where there is a flash it is possible to see the dark region of expanding gas just outside of the muzzle, and then about 1.-2. meters downstream the shock forms which initiates the flash burn within the first 10 milliseconds. The extent to which the flash spreads throughout the rest of the gas depends quite a bit on the amount of flash suppressant in the gas. Sometimes the flash is only a small region of luminosity which extinguishes itself very soon, and sometimes the flash consumes all of the gas and is very bright, extending over several meters.

We have obtained by hydrodynamical solutions for the gas and air outside of the gun for the cases $F = 1/2$ ($\theta = \pi/2$), $F = 1/4$ ($\theta = \pi/3$), and $F = 1/8$ ($\theta \simeq \pi/4$). To show the formation of the shock, we have plotted gas temperature versus radius at a fixed time for each of the three values of F (see Figure 6). Note how the gas cools very rapidly as it comes out of the muzzle and then at a distance of 1.5 - 2. meters the temperature raises back up to its initial value as a compression shock is formed. The unburned gas is then ignited and flash results. Note that the location of the shock region does not change greatly with a change in F. The fact that the shock distance at a given time

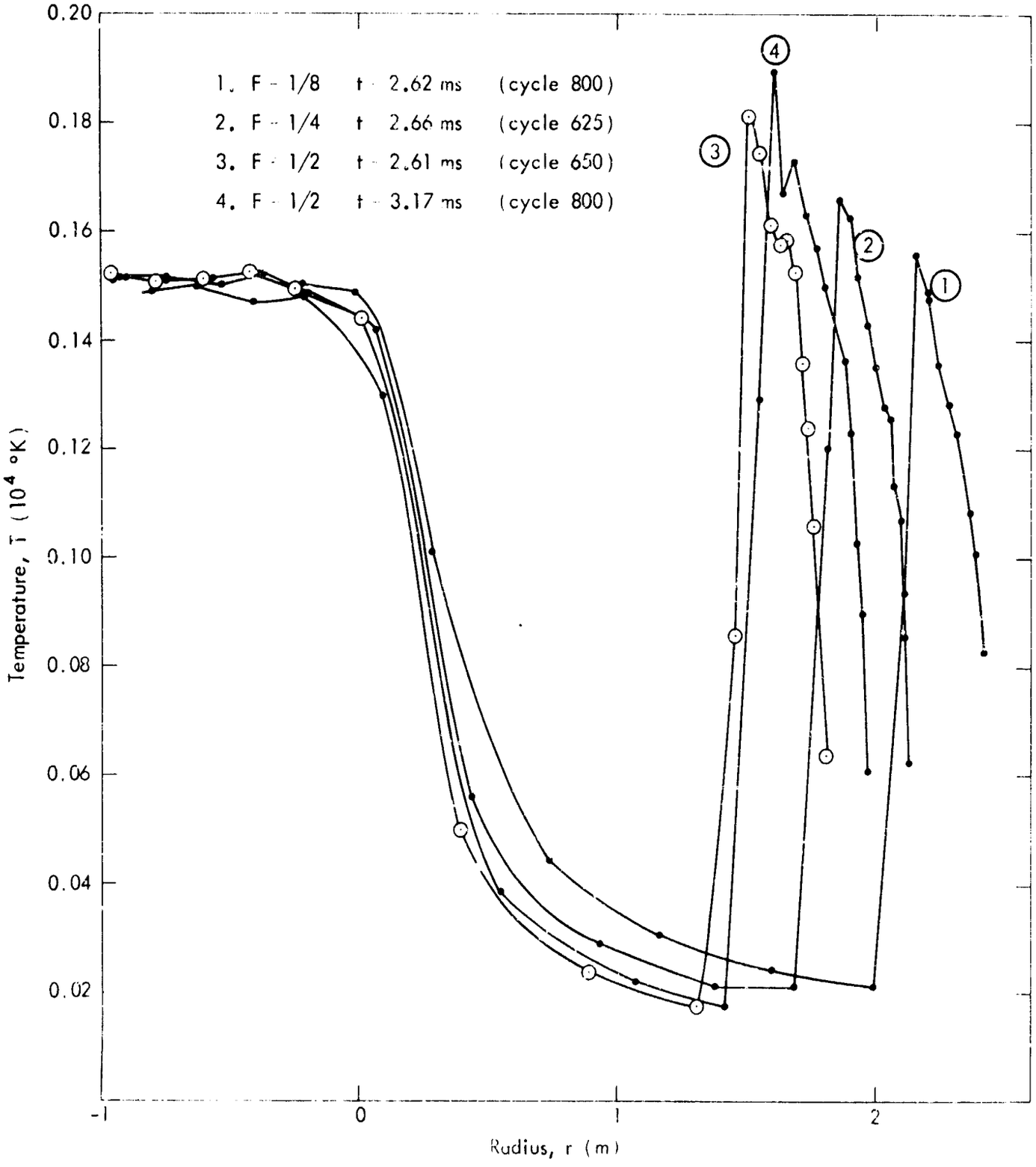

Fig. 6--Temperature-radius profiles for 5"/54 gun

is greater for smaller F shows that the gas moves faster when confined to a narrower cone. In addition to temperature, our calculations give the gas pressure, density, velocity and internal energy as a function of position and time.

In Figure 7 we have plotted the gas pressure (assuming F = 1/2) at a fixed distance from the muzzle (r = 2.m) versus time. Note the sharp rise in pressure as the gas first arrives at 2.m and the gradual decrease back to atmospheric pressure. This pressure-time history is in good agreement with corresponding experimental data,[3] except the experimental pressure curve usually drops somewhat below atmospheric and then forms a second peak of roughly the same magnitude as the first about 10 to 15 milliseconds later. Based on our experimental data, this second peak is due to the flash burning of the gas and it does not occur if there is no flash. The fact that we do not reproduce a second peak is probably due to the fact we do not burn the gas in the air properly, which would require knowledge of the exact chemical composition the gas and its mixing process with air. Also there are small instabilities in our numerical integration procedure, caused by the transition from plane geometry to conical geometry, which became larger with increasing time. These cause spurious oscillations in the pressure profile which would most likely obscure a second pressure peak even if it was caused by our burning procedure.

In Figure 8 we have plotted peak pressure versus radius using our calculations for the three angles $\theta = \pi/2$ (F = 1/2), $\theta = \pi/3$ (F = 1/4), and $\theta \simeq \pi/4$ (F = 1/8), along with the actual experimental data measured at these angles.[3] Note that we have made the assumption that the pressure at a given angle is obtained by using the value of F corresponding to that angle in the numerical integration. We feel that this is a rough approximation to the actual pressure distribution. Although the calculated pressures are greater than the corresponding experimental values by about 50%, they all lie on straight lines with almost the same slope, thus correctly reproducing the adiabatic expansion of the gas as it moves away from the muzzle. The fact that we have had to rely on separate calculations using different conical angles in order

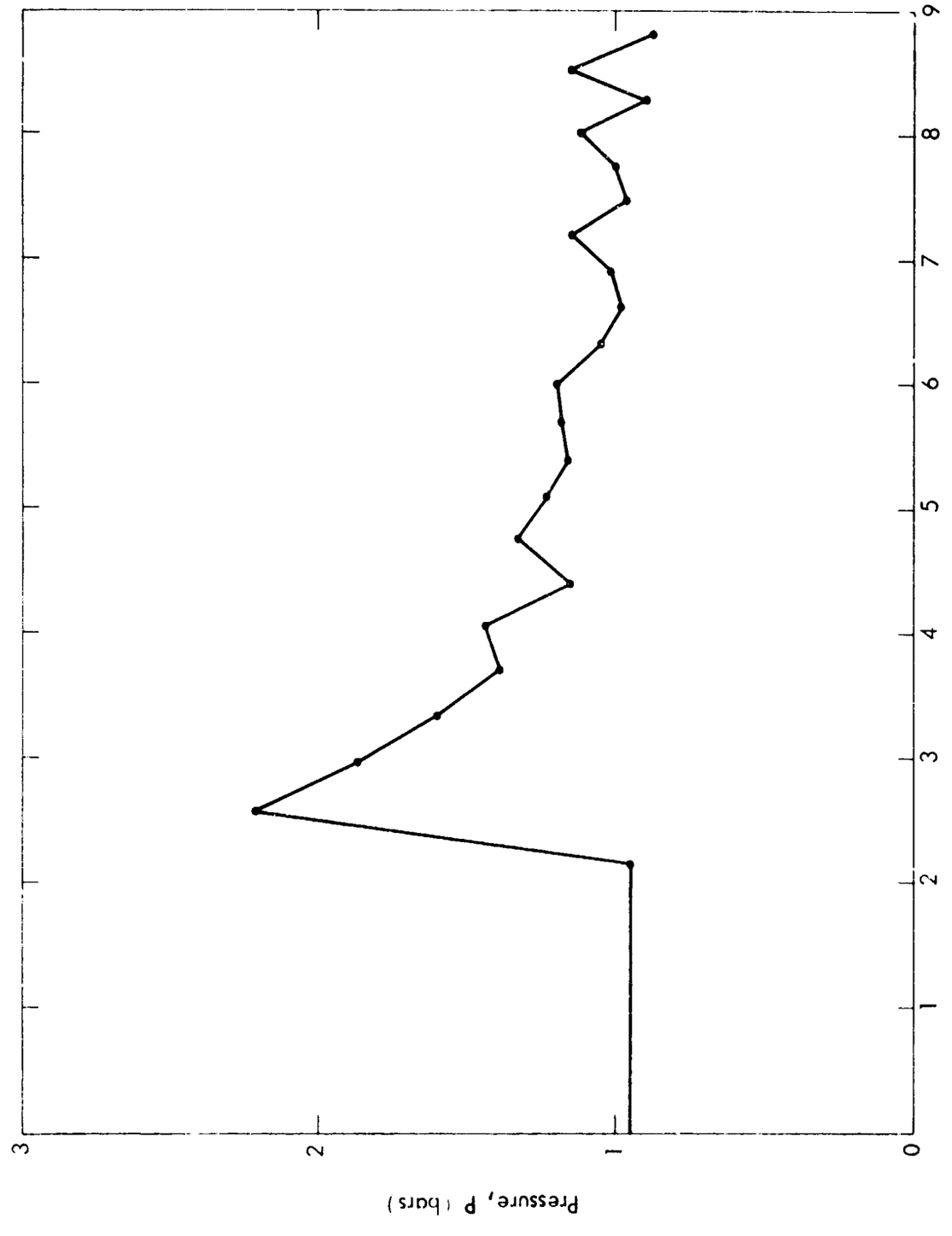

Fig. 7—Pressure-time profile for 5"/54 gun at r = 2m with F = 1/2

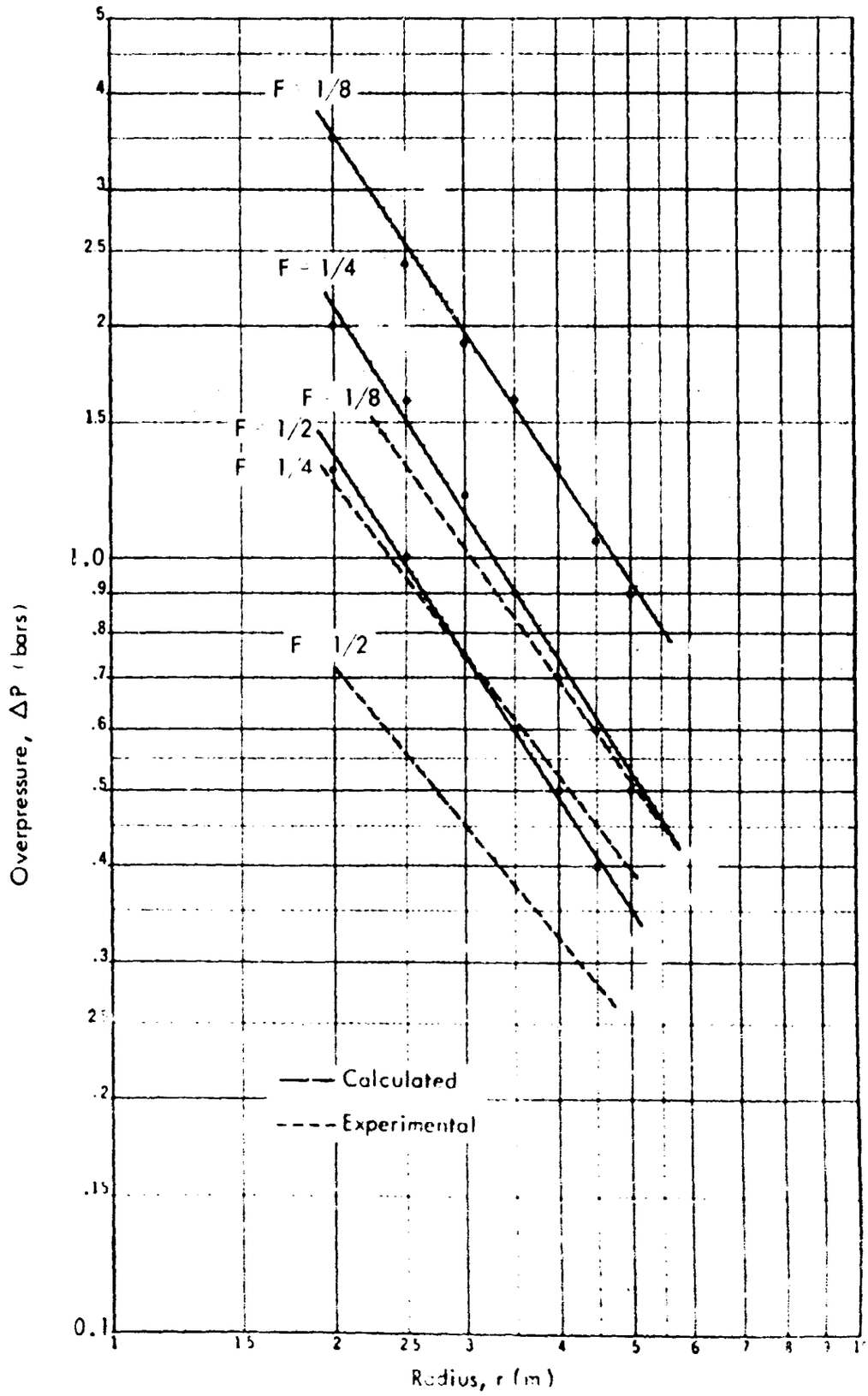

Fig. 8 — Peak overpressure versus radius for 5"/54 gun

to simulate the angular dependence of the pressure points up a major limitation in our one-dimensional conical calculations.

A final fact which comes out of our calculations is that the time for the pressure peak to travel from a radius r = 2m to r = 5m is roughly 6ms, which is in good agreement with the experimentally measured time.

IV. CONCLUSIONS

We have obtained a good quantitative model for the interior ballistics of large naval guns. Our results are limited by a number of simplifying assumptions but they are valid within these limitations. Our major improvement over previous treatments is the use of a more realistic equation of state for the propellant gas. We have shown how sensitive the interior ballistics are to a number of parameters. With more detailed experimental data we improve these parameters somewhat and also investigate the replacement of the various ideal assumptions by the actual physical process.

The flash and smoke are much more difficult to model in detail. Although our treatment accounts fairly well for the pressure distribution and shock reignition of the gas, we need a much better knowledge of the mixing of the gas and air and the flash burning mechanism. A number of the mathematical features of the hydrodynamics need to be improved. The use of two-dimensional calculations is necessary to provide for the angular dependence of the pressure. Alternate methods of treating the transition region between plane and conical geometry should be studied in order to improve the stability and accuracy of the calculations in that region.

We have established the validity of our calculations for large naval guns, but in order to show their general validity they should be applied to a variety of other guns.

APPENDIX

A study of some gun barrel effects which have a small but finite effect on the gas dynamics can be made by generalizing the Lagrangian equations of motion to include the effects of heat and mass transfer due to ablation and gas turbulence processes during the interior ballistics.

The equations of motion are recast in an "almost-Lagrangian" form which allows each of the zones to increase in mass as wall ablation occurs. Following the derivations of Crowley,[21] we obtain an equation of continuity

$$\frac{\partial \rho}{\partial t} = \frac{1}{V}\left(-\rho \frac{\partial V}{\partial t} + \dot{m} S_m\right) \tag{A-1}$$

where $\dot{m}$ is the mass flux (mass/area/time) and S_m is the surface area per unit mass. The momentum equation becomes

$$\frac{\partial u}{\partial t} = -\frac{\partial}{\partial m}(P + Q) + \dot{m} S_m (u_w - u) - \tau_w S_m \tag{A-2}$$

where u_w is the velocity of the mass entering a zone and τ_w is the shearing stress at the wall. The energy equation becomes

$$\frac{\partial E}{\partial t} = -(P + Q)\frac{\partial V}{\partial t} + \dot{m} S_m [(u-u_w)^2/2 + E_w - E] + \tau_w S_m |u| + \dot{H} \tag{A-3}$$

where the second term on the right hand side gives a rate of energy addition associated with the mass addition and E_w is the specific internal energy of the mass entering a zone. The third term comes from work done on a mass element by wall surface forces, and the fourth term, $\dot{H}$, is the rate at which heat is supplied to an element by turbulent heat transfer.

The following expression for the mass flux is used:

$$\dot{m} = \frac{q}{q^*} = \frac{C_H(\gamma Pu)/(\gamma-1)}{E_v + \eta(PV+E)} = \frac{C_H u}{\eta + E_v/(PV+E)} \tag{A-4}$$

where C_H is the dimensionless coefficient of heat transfer (the Stanton

PRECEDING PAGE BLANK

number), E_v is the sum of the enthalpy per unit mass required to heat the wall material to vaporization temperature, the specific heat of fusion and the specific heat of vaporization, and η is the turbulent transpiration coefficient. The source term, representing the heat lost from a zone due to the turbulent ablation process, is written as

$$\dot{H} = - q\, S_m = - C_H \rho (PV+E) u S_m \tag{A-5}$$

The shearing stress can be written as

$$\tau_w = \frac{1}{2} C_f \rho u^2 = C_H \rho u^2 \tag{A-6}$$

where C_f is the dimensionless coefficient of skin friction and $C_H = \frac{1}{2} C_f$ by the Reynolds analogy.[21]

To obtain a numerical solution we now put Eqs. (A-1) to (A-6) in difference equation form. Using

$$S^n_{m_{j-1/2}} = \pi D_e (X^n_j - X^n_{j-1}) = \frac{4}{D_e} V^n_{j-1/2} \Delta m^n_{j-1/2}, \tag{A-7}$$

$$\dot{m}^n_{j-1/2} = \frac{C_H \rho^n_{j-1/2} u^{n-1/2}_j}{\eta + E_v / (P^n_{j-1/2} V^n_{j-1/2} + E^n_{j-1/2})}, \tag{A-8}$$

$$\begin{aligned} \dot{H}^{n+1/2}_{j-1/2} &= - q^{n+1/2}_{j-1/2} S^{n+1/2}_{m_{j-1/2}} \\ &= - C_H \rho^n_{j-1/2} (P^n_{j-1/2} V^n_{j-1/2} + E^n_{j-1/2}) \\ &\quad \cdot u^{n+1/2}_j S^{n+1/2}_{m_{j-1/2}}, \end{aligned} \tag{A-9}$$

and

$$\tau^{n-1/2}_{w_j} = \frac{1}{2} C_f \cdot \frac{1}{2} (\rho^{n-1/2}_{j+1/2} + \rho^{n-1/2}_{j-1/2}) (u^{n-1/2}_j)^2, \tag{A-10}$$

and substituting into Eqs. (A-2) and (A-3) we obtain

$$u_j^{n+1/2} = u_j^{n-1/2} - \frac{\Delta t^n}{\Delta m_j^n}\left(P_{j+1/2}^n - P_{j-1/2}^n + Q_{j+1/2}^{n-1/2} - Q_{j-1/2}^{n-1/2}\right) \quad \text{(A-11)}$$

$$+ \left(u_j^{n-1/2} - u_w\right)\cdot\frac{1}{2}\left(\dot{m}_{j+1/2}^n S_{j-1/2}^n + \dot{m}_{j-1/2}^n S_{j-1/2}^n\right) \quad \text{(A-11)}$$

$$+ \tau_{w_j}^{n-1/2}\cdot\frac{1}{2}\left(S_{m_{j+1/2}}^n + S_{m_{j-1/2}}^n\right) \quad \text{(A-11)}$$

$$= u_j^{n-1/2} - \frac{\Delta t^n}{\Delta m_j^n}\left(P_{j+1/2}^n - P_{j-1/2}^n + Q_{j+1/2}^{n-1/2} - Q_{j-1/2}^{n-1/2}\right)$$

$$- \Delta t^n \frac{2C_H}{D_o}\left(u_j^{n-1/2}\right)^2\left[\frac{1}{\cdot\cdot + E_v/\left(P_{j+1/2}^n V_{j+1/2}^n + E_{j+1/2}^n\right)}\right.$$

$$\left. + \frac{1}{\cdot\cdot + E_v/\left(P_{j-1/2}^n V_{j-1/2}^n + E_{j-1/2}^n\right)} + 2\right]$$

and

$$E_{j-1/2}^{n+1} = E_{j-1/2}^n - \left[\frac{1}{2}\left(P_{j-1/2}^{n+1} + P_{j-1/2}^n\right) + Q_{j-1/2}^{n+1/2}\right]\left(V_{j-1/2}^{n+1} - V_{j-1/2}^n\right)$$

$$+ \frac{\Delta t^{n+1/2}\dot{m}_{j-1/2}^n S_{m_{j-1/2}}^{n+1/2}}{\Delta m_{j-1/2}^{n-1/2}}\left[\frac{\left(u_{j-1/2}^{n+1/2} - u_w\right)^2}{2} - E_{j-1/2}^{n+1/2} + E_w\right]$$

$$+ \frac{\Delta t^{n+1/2}}{2}\left(\tau_{w_j}^{n+1/2} + \tau_{w_{j-1}}^{n+1/2}\right)\frac{u_{j-1/2}^{n+1/2} S_{m_{j-1/2}}^{n+1/2}}{\Delta m_{j-1/2}^{n+1/2}} + \Delta t^{n+1/2}\frac{\dot{H}_{j-1/2}^{n+1/2}}{\Delta m_{j-1/2}^{n+1/2}}$$

$$= E_{j-1/2}^n - \left[\frac{1}{2}\left(P_{j-1/2}^{n+1} + P_{j-1/2}^n\right) + Q_{j-1/2}^{n+1/2}\right]\left(V_{j-1/2}^{n+1} - V_{j-1/2}^n\right)$$

$$+ \Delta t^{n+1/2}\frac{2C_H}{D_o} u_{j-1/2}^{n+1/2}\frac{1}{\cdot\cdot + E_v/\left(P_{j-1/2}^n V_{j-1/2}^n + E_{j-1/2}^n\right)}$$

$$\cdot\left[\frac{\left(u_{j-1/2}^{n+1/2}\right)^2}{2} - E_{j-1/2}^n + E_w\right] + \left(u_{j-1/2}^{n+1/2}\right)^2 - \left(P_{j-1/2}^n V_{j-1/2}^n + E_{j-1/2}^n\right)$$

where we have set $u_w = 0$.

We have followed Crowley and Glenn[22] in evaluating the constants for a steel shell moving down a steel barrel:

$C_H = .002$, $n = .2$, $E_w = 10$ jerks/Mg, $E_v = 12.5$ jerks/Mg.

To test the sensitivity of our results to these values we have varied C_H and E_w, which have the most effect on the results.

Results show the maximum breech pressure, P_{max}, lowered less than 2% in all cases and the muzzle velocity, u_{muz}, lowered by 1% for $C_H = .002$, $E_w = 10$ jerks/Mg; 2% for $C_H = .004$, $E_w = 10$ jerks/Mg; 10% for $C_H = .02$, $E_w = 10$ jerks/Mg and 4% for $C_H = .002$, $E_w = 20$ jerks/Mg and raised by 2% for $C_H = .002$ and $E_w = 5$ jerks/Mg. We thus have shown that the size of the ablation and turbulent heat transfer corrections is small.

REFERENCES

1. Siegal, A. E., "The Theory of High Speed Guns," NATO AGARDograph-91, U. S. Naval Ordnance Laboratory, Maryland, May, 1965. Included is a list of 117 related references.

2. Corner, J., Theory of the Interior Ballistics of Guns, John Wiley & Sons, Inc., New York, 1950.

3. Data on the guns studied was furnished by the U. S. Naval Weapons Laboratory, Dahlgren, Virginia, with the kind assistance of Dave Bowen, Charles Smith, Frank Kasdorf, and others, June, 1969. All of the data is recorded in NWL memos circa 1967-1968.

4. Corner, J., pp. 135-136, 340-342, 400.

5. von Neumann, J. and R. D. Richtmyer, J. Appl. Phys. 21, 232 (1950).

6. Brode, H. L., J. Appl. Phys. 26, 766 (1955).

7. Corner, J., p. 30.

8. Urbanski, T., Chemistry and Technology of Explosives, Clarendon Press, Oxford, 1965, Vol. II, p. 316.

9. Taylor, J. and C. R. L. Hall, J. Phys. and Col. . . m. 51, 593 (1947).

10. Corner, J., pp. 140, 146, 423.

11. Taylor, J., Detonation in Condensed Explosives, Clarendon Press, Oxford, 1952.

12. Jones, H. and A. R. Miller, Proc. Royal Soc. (London) 194A, 480 (1948).

13. Shear, R. E., "Detonation Properties of Pentolite," BRL Report No. 1159, Aberdeen Proving Ground, Maryland, December, 1961, Table 6.

14. Miller, R. O., "Estimating Caloric State Behavior in Condensed-Phase Detonations," from Detonation and Two-Phase Flow, ed. S. S. Penner and F. A. Williams, Academic Press, New York, 1962, p. 65.

15. Fickett, W., and W. W. Wood, Phys. Fluids 1, 528 (1958).

16. Corner, J., pp. 100-114.

17. Kamlet, M. J., and S. J. Jacobs, J. Chem. Phys. 48, 30 (1968).

18. For a detailed and complete description of the numerical integration procedure refer to H. L. Brode, W. Asano, M. Plemmons, L. Scantlin, and A. Stevenson, "A Program for Calculating Radiation Flow and Hydrodynamic Motion," The RAND Corporation, RM-5187-PR, April, 1967.

19. Corner, J., pp. 143-144.

20. Engineering Design Handbook, U. S. Army Material Command, February, 1965, Section 5-3.

21. Crowley, B.K., J. of Comp. Phys. 2, 61 (1967).

22. Crowley, B.K., and H.D. Glenn, "Numerical Simulation of a High-Energy (Mach 120 to 40) Air-Shock Experiment," Rept. UCRL-71470 (1969).

DOCUMENT CONTROL DATA

1. ORIGINATING ACTIVITY THE RAND CORPORATION	2a. REPORT SECURITY CLASSIFICATION: UNCLASSIFIED 2b. GROUP

3. REPORT TITLE

INTERIOR BALLISTICS AND GUN FLASH AND SMOKE

4. AUTHOR(S) (Last name, first name, initial)

Brode, H. L., Enstrom, J. E.

5. REPORT DATE	6a. TOTAL NO. OF PAGES	6b. NO. OF REFS.
October 1969	47	22

7. CONTRACT OR GRANT NO.	8. ORIGINATOR'S REPORT NO.
F44620-67-C-0045	RM-6127-PR

9a. AVAILABILITY/LIMITATION NOTICES	9b. SPONSORING AGENCY
DDC-1	United States Air Force Project RAND

10. ABSTRACT

An investigation of the gas dynamics of various large naval guns, including the interior ballistics (charge burning, propellant gas expansion and shell acceleration) and the nature of the gas expansion and air shock beyond the muzzle. Solutions are accomplished by a numerical program which integrates the partial differential equations appropriate to the gas dynamics in one space dimension. The equations of state for the gas and air are treated in some detail, as is the nature of the charge burn, the barrel friction, and the shell inertia. The dynamics of the partially burned charge gases which sometimes flash burn after ejection from the muzzle are treated with the limits of expansion into various conical geometries. Comparisons are made with observations of both the interior ballistics and of the smoke, flash, and blast from the exhaust.

11. KEY WORDS

Ordnance
Artillery
Gas dynamics
Numerical methods and processes
Detection
Radar